scientific reports

Check for updates

OPEN

Single cell analysis of diverse immune cell in pneumococcal meningitis

Yujie Zhang, Jing Duan, Sufang Lin, Jialun Wen & Jianxiang Liao✉

***Streptococcus pneumoniae*, a Gram-positive, human-specific commensal infectious pathogen, poses a significant global health threat, especially in children under five, often resulting in fatalities. The intricacies of the immune response in pneumococcal meningitis (PM) remain elusive, necessitating a meticulous examination of immune cell subsets at the single-cell resolution. In this study, we performed single-cell RNA sequencing of peripheral blood mononuclear cells from PM patients and healthy individuals. We found significant relative changes in the compositions of immune cell subset, with significant relative increases in platelets, neutrophils, and their precursors, alongside relative decreases in natural killer (NK) cells, T cell subtypes, and plasmacytoid dendritic cells in PM patients. Functional enrichment analyses revealed an up-regulation of neutrophils-related immune genes across multiple immune cell types, including platelets, myeloid cells and B cells, suggesting excessive neutrophil activation. However, a down-regulation of genes involved in antigen processing and presentation in myeloid cells and B cells in the PM group indicated a relative dampening of the adaptive immune response in the PM patients. This was further corroborated by the reduced proportions of plasmacytoid dendritic cells and T cells. Furthermore, genes involved in cytotoxity were down-regulated in both NK cells and T cells, alongside impaired T cell activation. Notably, distinct B cell subtypes, including unique naïve B cell clusters, demonstrated differentially expressed genes associated with both innate and adaptive immune responses. In conclusion, our study provides a comprehensive single-cell transcriptomic landscape of immune responses in PM. The identified cellular and molecular signatures offer potential targets for therapeutic intervention and provide a foundation for further investigation into the immunopathogenesis of pneumococcal meningitis.**

Keywords Pneumococcal meningitis, RNA sequencing, Platelets, Neutrophils, T cells, B cells

Abbreviations

PBMC	Peripheral blood mononuclear cells
DEGs	Differentially expressed genes
PM	Pneumococcal meningitis
scRNA-seq	Single-cell RNA sequencing
GO	Gene Ontology (GO)
KEGG	Kyoto Encyclopedia of Genes and Genomes
pDCs	Plasmacytoid dendritic cells
MPs	Mononuclear phagocytes
ClassicalMO	Classical monocytes
GDT cells	Gamma delta T cells
PAFR	Platelet-activating factor receptor
NET	Neutrophil extracellular trap
TLR	Toll-like receptor
NOD	Nucleotide oligomerization domain
TNF	Tumor necrosis factor
CSF	Cerebrospinal fluid

Streptococcus pneumoniae (pneumococcus) is a Gram-positive, human-specific commensal bacterium residing in the upper respiratory tract. However, it can occasionally escalate into a severe health threat particularly

Department of Neurology, Shenzhen Children's Hospital, No. 7019 Yitian Road, Futian District, Shenzhen, China. ✉email: epilepsycenter@vip.163.com

for children, the elderly, and immune-deficient individuals. Pneumococcal meningitis (PM) occurs when pneumococcus crosses the blood–brain barrier, triggering an inflammatory response that induces brain damage[1]. PM is the primary etiologic agent of bacterial meningitis and a significant cause of morbidity and mortality in infants and children, with mortality rates hovering between 10.4 and 11.4% and sequelae rates as high as 30–50%[2]. Despite the development of effective antibiotics and vaccines for PM, the mortality rate of PM remains high[3]. PM induces acute, purulent inflammatory response upon infection. Numerous studies have shown that both the innate and the adaptive immunity play an essential role in the inflammatory response to pneumococcus in PM patients[4]. Therefore, a comprehensive understanding of immune responses in PM patients may be of clinical significance for PM therapies and diagnosis.

The onset of pneumococcus infection results in activation of the immune response, but *S. pneumoniae* also produces toxins that hinder the host's immune system response, thus escaping from the defense mechanisms[5]. Studies have proved a connection between innate immune cells and pneumococcal infections[4]. During PM, a robust influx of neutrophils is recruited[6,7]. However, recent studies have shown that the excessive neutrophil activity may hinder the bacterial clearance during PM. As early as 1995, it was recognized that the platelet-activating factor (PAF) receptor (PAFR) serves as a ligand for *S. pneumoniae*, and clinical observations have linked increased platelet counts to pneumonia patients[8–10]. Moreover, some studies found that the lower platelet count is predictive of mortality in PM cases[11,12]. The function of NK cells against *S. pneumoniae* infections remains relatively underexplored. Two reports found that the elevated NK cell activity during pneumococcal pneumonia results in adverse outcomes[13,14]. Adaptive immune responses have also been reported in PM patients. The early adaptive immune response delays the spread of pneumococci from the brain to the systemic circulation and shapes the immune response[15]. γδ T cells accumulate, activate and support pneumococcal clearance during *S. pneumoniae* infections[16,17]. Recent studies also showed the naturally acquired adaptive immunity against pneumococci in humans, mediated by IgG antibodies and Th17 cells. Notably, B cells produce natural IgM antibodies against pneumococci by improving the complement-mediated systemic immunity[18,19].

In the present study, we comprehensively profiled the immune responses in PM patients by single-cell RNA sequencing (scRNA-seq) of peripheral blood mononuclear cells (PBMCs). This approach aimed to identify the key immune cell subsets and underlying mechanisms of *S. pneumoniae*-induced immune response in PM patients.

Materials and methods

Sample collection

The PBMCs were collected from three patients (10.3 months old) admitted to Shenzhen Children's Hospital, diagnosed with PM caused by *S. pneumoniae* infection. The control PBMC samples were collected from individuals determined to be healthy in physical examinations (48.3 months old) conducted at Shenzhen Children's Hospital. All participants were enrolled from January 2021 to June 2021. This study and all methods were approved by the institutional ethics committee of Shenzhen Children's Hospital, and informed consent was obtained from parent and/or legal guardian for study participation. Detailed clinical information of the participants is summarized in Supplementary Table S1. We confirm that all methods were performed in accordance with the guidelines by the institutional ethics committee of Shenzhen Children's Hospital.

Sample suspension processing

Immediately after collection, blood samples were transported to the Singleron lab at a controlled temperature of 2–8 °C. PBMCs were isolated by density gradient centrifugation using Ficoll-Paque Plus medium (GE Healthcare) and washed with Ca/Mg-free PBS. 2 mL of GEXSCOPE red blood cell lysis buffer (RCLB, Singleron) was added at 25 °C for 10 min to remove the red blood cells. The solution was then centrifuged at 500g for 5 min and re-suspended in PBS. The blood samples were centrifuged at 400g for 5 min at 4 °C, and the supernatant was discarded. After removal of red blood cells, PBMCs were isolated by centrifugation at 400g for 10 min at 4 °C. The supernatant was discarded and the PBMCs were resuspended in PBS to obtain a single-cell suspension. Finally, the samples were stained with Trypan Blue and cell viability was evaluated under a microscope.

Single-cell RNA sequencing of PBMCs

The single-cell suspensions (2×10^5 cells/mL) in PBS (HyClone) were prepared and loaded into microfluidic devices. Following the manufacturer's protocol (Singleron Biotechnologies), scRNA-seq libraries were constructed using the GEXSCOPER Single-Cell RNA Library Kit[20]. Subsequently, each library was diluted to a concentration of 4 nM and sequenced on the Illumina HiSeq X platform, generating150-bp paired-end reads for comprehensive analysis.

Primary analysis of raw data

The raw reads from scRNA-seq were processed by the CeleScope (https://github.com/singleron-RD/CeleScope) v1.17 pipeline to generate gene expression matrixes. First, low-quality reads were removed with Cutadapt v1.17[21]. Poly-A tails and adapter sequences were trimmed, and cell barcodes and UMI were extracted. Then, the STAR v2.6.1a was used to map the reads to the reference genome GRCh38 (ensembl version 92 annotation)[22]. Following this, UMI counts and gene counts of each cell were acquired with the feature Counts v2.0.1 program[23], and expression matrix files were generated for further analysis.

Quality control, dimension-reduction and clustering

Cells with gene counts below 200 or with top 2% gene counts, as well as those with the top 2% UMI counts were filtered out to ensure data quality. These cells were excluded from further analysis. To proceed, we used Seurat v3.1.2 for dimension reduction and clustering[24]. The NormalizeData and ScaleData functions were used to

normalize and scale all gene expression values, respectively, ensuring uniformity across the dataset. To identify the most informative genes for principal component analysis (PCA), we employed the FindVariableFeatures function to select the top 2000 variable genes. The top 20 principal components were used to separate cells into multiple clusters with FindClusters. Harmony was used to remove batch effect between samples[25]. Finally, for visualization purposes, we projected the cells onto a two-dimensional space with Uniform Manifold Approximation and Projection (UMAP) algorithm.

Differentially expressed genes (DEGs) and cell type annotation

DEGs were identified by the Seurat FindMarkers function based on the Wilcoxon likelihood-ratio test with default parameters. To qualify as a DEG, the genes had to be expressed in more than 10% of the cells within a cluster and with an average log (Fold Change) value exceeding 1. Cell types were identified based on the expression of canonical markers found in the DEGs using the SynEcoSys database. Doublet cells that expressed markers characteristic of multiple cell types, were removed from subsequent downstream analysis.

Pathway enrichment analysis and trajectory analysis

Gene Ontology (GO) and Kyoto Encyclopedia of Genes and Genomes (KEGG) pathway analyses were performed using the "clusterProfiler" R package 3.16.1[26], to investigate the potential functions of DEGs[27–29]. Terms with corrected p value (p adjust) < 0.05 were considered as significantly enriched. The Monocle2 tool was used to reconstruct cell differentiation trajectories[30]. Additionally, we refined our analysis by applying the FindVairableFeatures functions and utilizing DDRTree for Dimensionality Reduction. The trajectory was visualized by the plot_cell_trajectory function. CytoTRACE was used to predict the differentiation potential of monocyte subpopulations[31].

U cell scoring

We performed gene set scoring with the R package uCellv 1.1.0[32]. The U Cell scores were calculated from the ranking of each gene according to its expression in each cell, using the Mann–Whitney U test.

Statistics and repeatability

Statistical analysis was performed using unpaired two-tailed Wilcoxon rank-sum tests, paired two-tailed Wilcoxon rank-sum tests and unpaired two-tailed Student's *t* test. All statistical analyses and presentation were performed using R. $P < 0.05$ was considered as statistically significant.

Ethics statement

The studies involving human participants were reviewed and approved by the institutional ethics committee of Shenzhen Children's Hospital. Informed consent was obtained from parent and/or legal guardian for study participation.

Results

Single-cell sequencing datasets from blood samples of PM patients

To identify the immunological feature of PM, we performed scRNA-seq of PBMCs of 3 meningitis patients infected with *S. pneumoniae* and 3 healthy control individuals (Supplementary Table S1). The experimental procedure is shown in Fig. 1A. We obtained 20,966 cells in the PM group, and 17,353 cells in the control group, all of which passed quality control measures. The detailed information on quality control measures is shown in Supplementary Table S2.

After preliminary unsupervised clustering and annotation by the typical marker genes, 10 cell types were identified in both PM and control groups (Fig. 1B, C, S1; Supplementary Table S3), including NK cells, T cells, B cells, plasma cells, plasmacytoid dendritic cells (pDCs), neutrophils, proneutrophils, mononuclear phagocytes (MPs), platelets, and erythrocytes. However, the relative proportions of these 10 cell types varied considerably between the PM and the control groups (Fig. 1D). Specifically, the PM group exhibited a significant relative increase in the proportion of platelets ($p < 0.05$), neutrophils ($p = 0.0557$), and proneutrophils ($p < 0.05$), coupled with a significant relative decrease in the proportions of NK cells ($p < 0.001$), pDCs ($p < 0.001$), and T cells ($p < 0.01$). These observations point to a distinct immune cell subset composition in PM patients, which may have implications for the pathogenesis of the disease.

Immunological features of platelets in PM patients

Platelets, traditionally recognized for their pivotal role in hemostasis and thrombosis, have emerged as critical players in the immune defense against bacterial infections, as evidenced by recent research[33]. Our investigation uncovered a significant relative increase in platelet counts in the PM group (Fig. 1D, $p < 0.05$), prompting a detailed analysis of DEGs within these cells. We identified 825 up-regulated and 703 down-regulated DEGs between the PM and control groups, with several up-regulated genes associated with the immune response, including *ALOX5*, *MMP9*, *S100P*, *FCGR3B*, *FCGR2A*, *TLR4*, *TLR2*, and *ALOX5AP* (Supplementary Fig. S2A, Supplementary Table S4-1).

GO functional enrichment analysis revealed that the up-regulated genes were mainly enriched in the biological processes of neutrophils (Fig. S2B, Supplementary Table S5). KEGG analysis revealed that the up-regulated DEGs were enriched in the chemokine signaling pathway, B cell receptor signaling pathway, and neutrophil extracellular trap (NET) formation pathway (Fig. S2C, Supplementary Table S5). The up-regulated *ALOX5*, *MMP9*, *S100P* and *FCGR3B* were involved in pathways of neutrophil-related biological processes, while *FCGR3B*, *FCGR2A*, *TLR4*, and *TLR2* were involved in NET formation. The up-regulated *LILRB2*, *LILRB3*, and *MAPK14* mediated B-/T-cell receptor signaling.

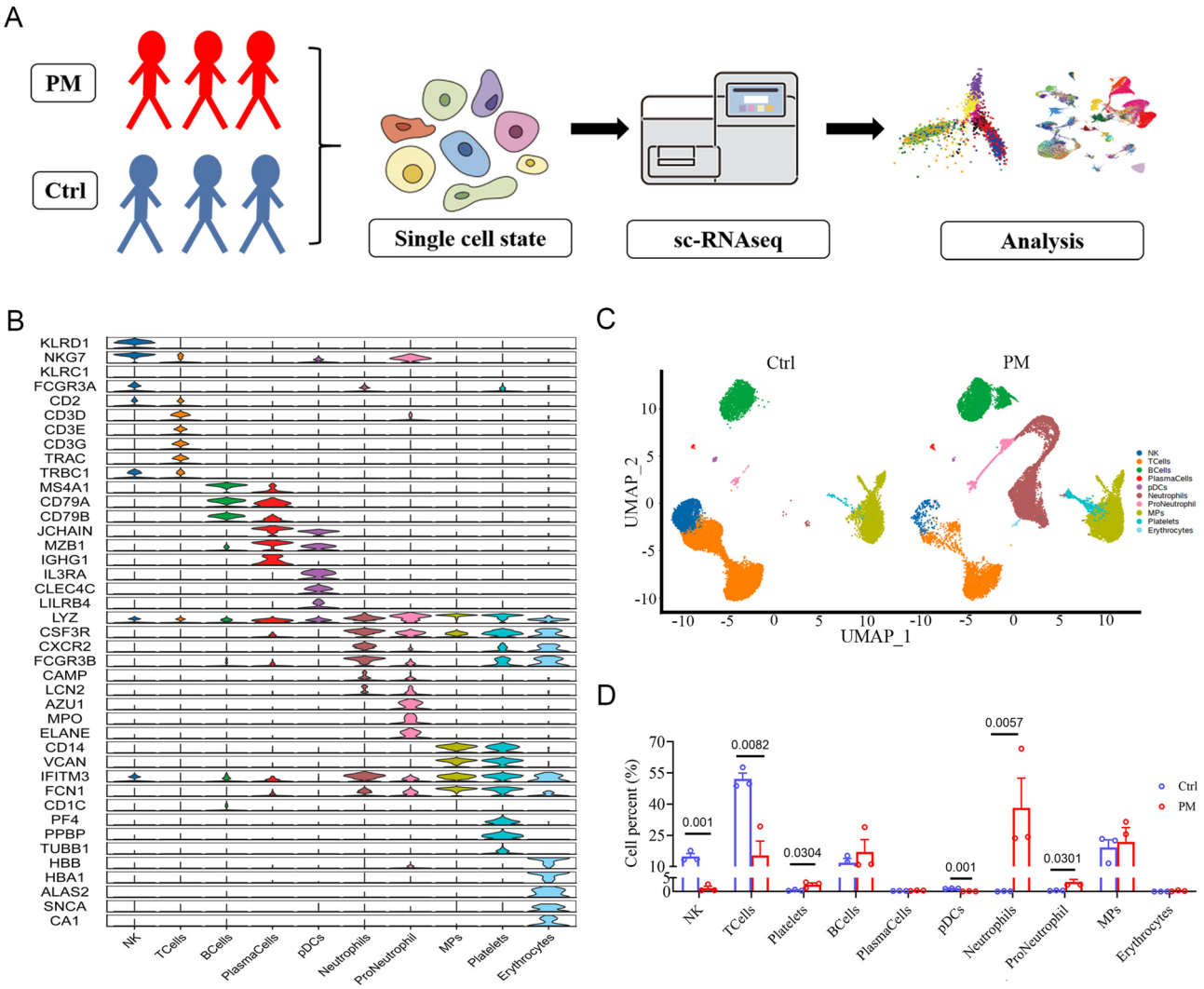

Fig. 1. Characterization and clustering of single cells in the PM and the control groups. (**A**) Schematic of the study design. Three healthy individuals and three patients were enrolled in the control and PM groups, respectively (PM, $n = 3$; control, $n = 3$). (**B**) Violin plot of canonical marker genes for each cell type. Different colors represent different cell types. (**C**) UMAP dimensionality-reduction projection analysis of the PM and control groups. Cell types coded by different colors, and each dot corresponds to a single cell. (**D**) Comparison of the relative proportions of each cell subtype between the PM and the control groups. Comparisons were made using two-tailed unpaired Student's t-test and the p-values are not adjusted for multiple comparisons. Data are shown as the mean ± SEM.

To delve deeper into the role of platelet subtypes in PM, we identified five distinct subtypes based on characteristic gene expression patterns, with platelet subtype 2 being unique to the PM group (Fig. 2A, B). Compared with the other subtypes, *ALOX5AP*, *S100P*, *FCGR3B*, *MMP9*, and *CMTM2* were the top five up-regulated genes in platelet subtype 2 (Fig. 2C). Further enrichment analysis of the representative up-regulated DEGs between platelet subtype 2 and other subtypes was performed firstly, with up-regulated DEGs implicated in the biological processes of neutrophils (Fig. 2D), which was consistent with the results of the enrichment analysis of total platelets (Fig. S2B). KEGG analysis identified the involvement of these DEGs in inflammatory and immune pathways (Fig. 2E). The gene set pathway enrichment score for platelet subtype 2 was higher in both inflammatory response and IL6–JAK–STAT3 signaling pathways, which are known regulators of platelet aggregation and activation[34] (Fig. 2F). In addition, to ensure the robustness of our findings, we performed additional analyses and included UMAP plots in Supplementary Figure S2D and S2E, demonstrating that the clustering results remain consistent even after removing neutrophil and other contaminant genes. This confirms the distinct presence of platelet subtype 2 in the PM group and supports the reliability of our conclusions.

Trajectory analysis of platelets revealed three distinct developmental trajectories, with subtype 2 marking the end of the differentiation spectrum, significantly correlated with its distinctive presence in the PM group (Fig. 3A–C). Beam analysis identified five differentially expressed gene clusters, with cluster 2 consistently enriching key genes (Fig. 3D). The pseudotime gene expression distribution further confirmed the increased

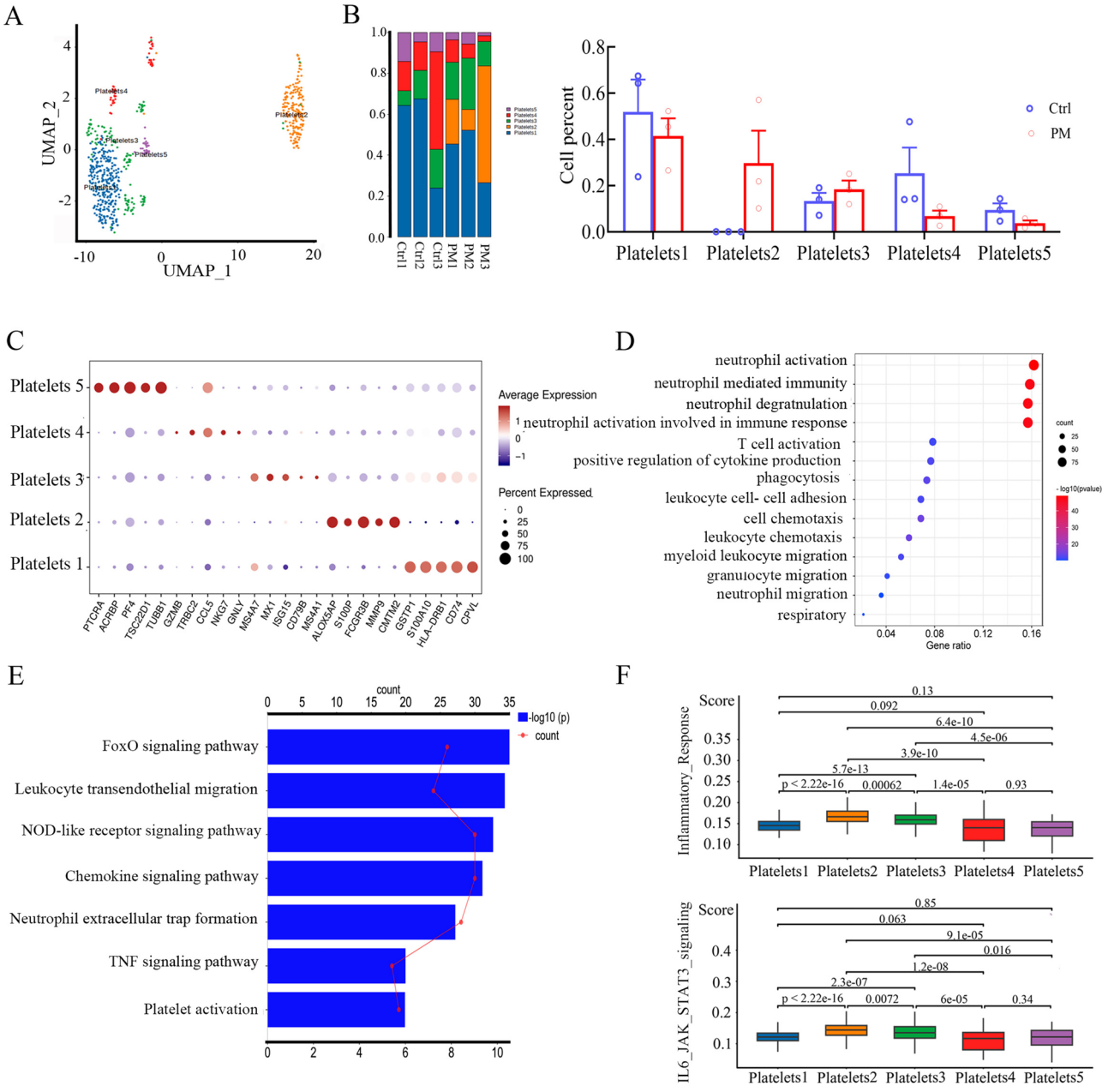

Fig. 2. The immunological characteristics of platelets in PM. (**A**) UMAP plot of platelet subtypes. Cell subtypes coded by different colors, and each dot corresponds to a single cell. (**B**) The relative proportions of each platelet subtype in each sample (left) and comparison of platelet subtypes between PM and control groups (right). (**C**) Dot plot for the top 5 DEGs of each platelet subtype. The average normalized expression is used to show the relative strength of gene expression compared to other subtypes, while the size of the dot indicates the percentage of cells within the cell subtype that express that marker. The horizontal axis displays the names of the genes, with red color used for the top 5 DEGs. The vertical axis indicates the cell subtype. (**D**) GO enrichment analysis of DEGs between platelet subtype 2 and other platelet subtypes. Pathways are displayed on the vertical axis. At the bottom, the proportion of DEGs that are annotated to the pathway relative to the total number of DEGs in platelet subgroup 2 is indicated. The size of the dot represents the proportion of DEGs in each pathway. (**E**) KEGG enrichment analysis of DEGs between platelet subtype 2 and other platelet subtypes. The vertical axis displays the enriched pathways. The length of the bars indicates the significance of the enrichment results, where longer bars indicate more significant enrichment. The points on the red line represent the −log10 (p.adjust) values, as shown on the bottom horizontal axis. The top horizontal axis represents the number of genes enriched in each pathway. (F) Gene set analysis of different platelet subtypes in both inflammatory response (upper) and the IL6–JAK–STAT3 signaling pathways (bottom). The vertical axis represents the U cell score, while the horizontal axis displays the different platelet subtypes. Pairwise comparisons were made between each pair of subtypes. Wilcoxon rank-sum test was performed, with $p < 0.05$ was considered as statistically significant.

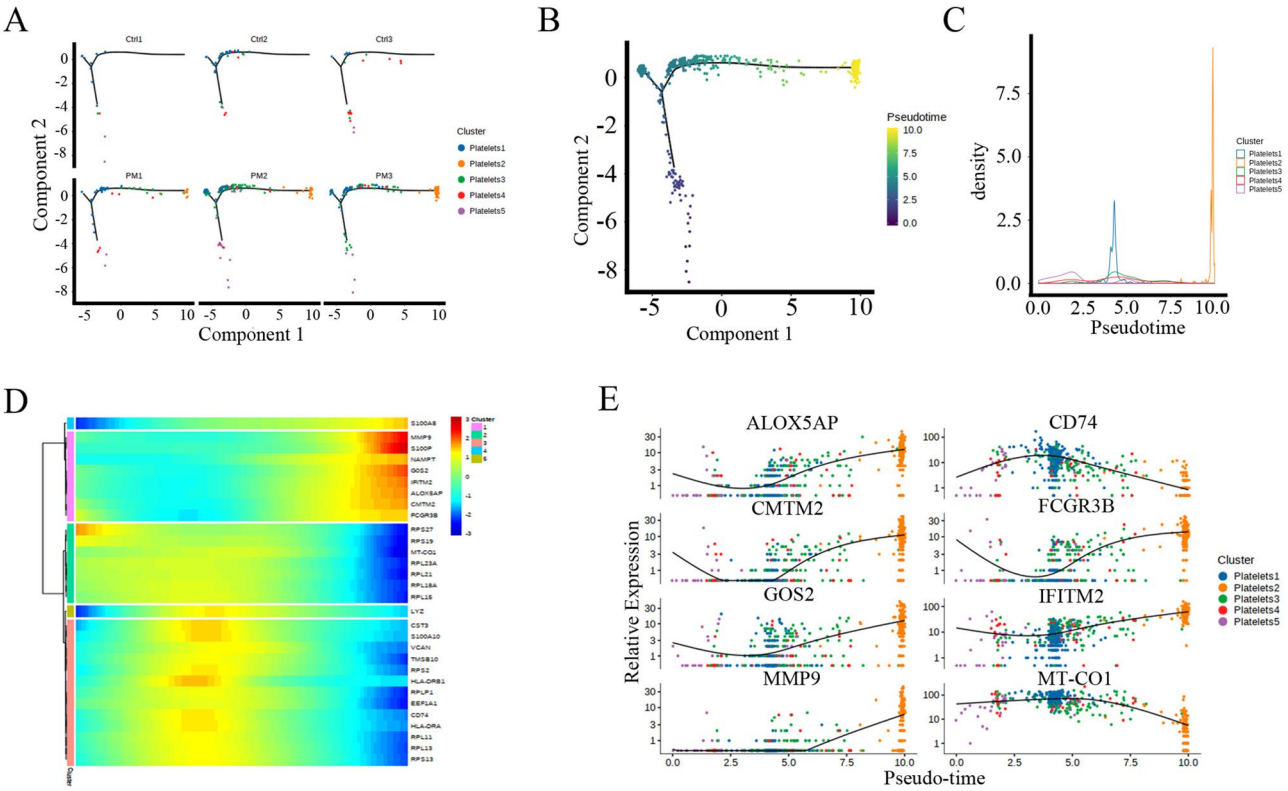

Fig. 3. The trajectory analysis of platelets. (**A**) Pseudotime trajectory analysis of platelet subtypes in each individual. Different colors indicate different cell types in each sample. (**B**) Pseudotime trajectory analysis of all cells. The time sequence indicates the pseudotime sequence of differentiation. (**C**) Cell densities along the pseudotime. (**D**) Dynamics of gene expression along the pseudotime. The abscissa indicates time, while the ordinate indicates the gene. (**E**) Expression of top 8 genes over pseudotime. Different colors indicate different cell types in each sample.

expression of *ALOX5AP*, *FCGR3B*, and *MMP9* within platelet cluster 2 (Fig. 3E). Altogether, these results indicated that platelet play a distinct role in pneumococcal meningitis, characterized by the unique presence of platelet subtype 2 and significant up-regulation of genes implicated in neutrophil activation and immune response pathways.

Immunological features of myeloid cells in PM patients

Myeloid cells are crucial for the innate immune response to bacterial infections, and our study focused on the roles of monocytes and dendritic cells in PM. Utilizing characteristic marker genes, we discerned four myeloid cell clusters in both PM patients and controls: classical monocytes (ClassicalMO), non-classical monocytes (Non-classicalMO), conventional dendritic cells (cDCs), and plasmacytoid dendritic cells (pDCs) (Fig. 4A). Notably, the ClassicalMO cluster was enriched in the PM group, while the abundance of both dendritic cell clusters was relative decreased in the PM group (Fig. 4B, C).

Through a meticulous examination of DEGs across these clusters, we performed enrichment analyses to uncover the immunological implications (Fig. 4D, F, H, J, Supplementary Table S4-3). GO enrichment analysis showed that the upregulated DEGs across all four clusters were significantly involved in the neutrophil-related biological processes (Fig. 4E, G, I, K). Additionally, KEGG pathway analysis indicated that DEGs from both Non-classicalMO and cDC clusters were enriched in the IL17 signaling pathway and NOD-like receptor signaling pathway (Fig. S3), with specific pathways for ClassicalMO and pDC clusters detailed in Fig. S3.

Moreover, both GO and KEGG enrichment analyses revealed that down-regulated DEGs were enriched in antigen processing, presentation, and T cell activation pathways within the ClassicalMO cluster (Fig. 4E, S3B). In addition, these DEGs were also enriched in antigen processing and presentation pathways in both non-classicalMO and pDC cells (Fig. S3B). At last, the cDC cluster showed down-regulated DEGs that mediated T-cell differentiation and were enriched in TNF and Toll-like receptor (TLR) signaling pathways (Fig. 4K, S3B), with detailed information provided in Supplementary Table S6. Our analysis of myeloid cells in PM patients reveals a complex pattern of gene regulation in PM patients, with specific clusters exhibiting both upregulation and downregulation of genes critical to immune cell functionality.

Neutrophil gene expression profiling reveals enhanced immune response mechanisms in neutrophil and proneutrophil cells in PM patients

Neutrophils, the predominant leukocytes population, constitute the first line of defense against bacterial and fungal infections within the immune system. In our study, a higher relative proportion of neutrophils and their precursors, the proneutrophils, was observed in the PM group compared to the control group (Fig. 1D). To further investigate the role of neutrophils in PM infection, we analyzed DEGs of combined neutrophils and proneutrophils between the PM and the control groups. This analysis yielded 1281 upregulated and 1795 downregulated DEGs (Fig. 5A, Supplementary Table S4-4). Notably, several upregulated DEGs in the PM group are integral to immune response mechanisms, such as *FPR1, FPR2, C5AR1, CXCR1, CXCR2, ITGB2, ITGAM, SELL, SELPLG, FCGR2A, FCGR3B,* and *FCGRT*. These genes encode key chemoattractant receptors, adhesion molecules, and IgG receptors. In addition, these genes play a crucial role in neutrophil function, including migration, recognition, and interaction with other immune cells.

GO functional enrichment analysis revealed that over 200 upregulated DEGs were significantly involved in neutrophil biological processes (Fig. 5A and Supplementary Tables S4-4 and S7). Both GO and KEGG analyses concurred, demonstrating that these upregulated DEGs were enriched in phagocytosis, cytokine production, and pattern recognition receptor signaling (PRRs) pathway (Fig. 5B). Further corroborating these findings, KEGG pathway analysis showed an enrichment of DEGs in the NET formation pathway, NOD-like receptor signaling pathway and platelet activation, all of which are indispensable for the orchestration of innate immune response (Fig. 5B). In addition, we analyzed the interaction between neutrophils and platelets and found an increased interaction in the PM group (Fig. S4A). Our analysis highlights the significant upregulation of genes in neutrophils associated with key immune response pathways in PM, indicating a robust activation state characterized by enhanced phagocytosis, cytokine production, and pathogen recognition.

Impaired Functionality of NK Cells in PM patients

NK cells, pivotal cytotoxic lymphocytes of the innate immune system, are essential for controlling intracellular pathogens by releasing them into the adaptive cell-mediated immune response[35,36]. The detailed analysis of DEGs between the PM and the control groups is shown in Supplementary Table S4-5. In our study, a significantly reduced proportion of NK cells was observed in the PM group compared to the control group, underscoring the critical involvement of NK cells in PM (Fig. 1D).

GO functional enrichment analysis of the downregulated DEGs in NK cells revealed significant enrichment in biological processes, including cell–cell adhesion, T-cell activation, and NK cell activation pathways (Fig. 5C, D, Supplementary Table S4-5, Supplementary Table S8). Furthermore, KEGG analysis indicated that these downregulated DEGs in NK cells are enriched in key pathways, including the TNF signaling pathway, TLR signaling pathway, apoptosis, and the T cell differentiation pathway (Fig. 5D, Supplementary Table S8). These data suggest that the functionality of NK cells is impaired in PM.

T cell subtype-specific gene regulation and immune pathway involvement in PM

To elucidate the role of T cells in PM, we categorized these T cells into five distinct subtypes based on their lineage and functional status: gamma delta T (GDT) cells, CD8 + effector T (CD8 Teff) cells, CD4 + naïve T cells, CD8 + naïve T cells, and hematopoietic stem cells (HSCs) (Fig. 6A). Notably, the PM group exhibited a diminished presence of both GDT and CD8 Teff cells compared to the control group (Fig. 6B). We first analyzed the DEGs of GDT cells between the PM and control groups (Fig. 6C, Supplementary Table S4–7).

GO functional enrichment analysis showed that the downregulated DEGs in GDT cells were significantly enriched in immunity-related pathways, including regulation of T cell- or lymphocyte-mediated immunity, adaptive immune response, and cytotoxicity (Fig. 6D). However, the upregulated DEGs were enriched in processes involving protein targeting to the ER pathway (Fig. 6D). Furthermore, KEGG pathway analysis highlighted the enrichment of downregulated DEGs in pathways like TNF signaling, antigen processing and presentation, and the TLR pathway (Fig. 6E). In the case of CD8 Teff cells, down-regulated DEGs (Fig. 6F, Supplementary Table S4-7) were significantly enriched in processes related to viral transcription and mRNA catabolism, while up-regulated DEGs were linked to neutrophil functions, such as activation and degranulation (Fig. 6G). KEGG analysis indicated that downregulated genes were significantly enriched in pathways like TNF signaling, IL-7 signaling, and B cell receptor signaling (Fig. 6H).

Furthermore, gene set pathway enrichment score analysis revealed that both GDT and CD8 Teff cells displayed significantly higher scores than other T cell subtypes in MHC-II signaling and T-cell inflamed signaling pathways, indicating their heightened involvement in the immune response (Fig. 6I, J). Additionally, the scores for both GDT and CD8 Teff cells were significantly elevated in the PM group compared to the control group (Fig. S4B and S4C). A detailed account of the GO and KEGG functional analyses conducted for the DEGs between the PM and control groups is provided in Supplementary Table S9. Altogether, our results reveal a noteworthy suppression of genes essential for T cell functionality and antigen presentation, suggesting the dampened T cell response in patients afflicted with pneumococcal meningitis.

Immunological features of B cells in PM patients

To discern the distinctive attributes of B cells within the context of PM, we first performed enrichment analysis of DEGs in B cells between PM and control groups (Fig. S5A, Supplementary Table S4-8). We found that an intriguing enrichment of upregulated DEGs in B cells, specifically those involved in the biological processes associated with neutrophils (Fig. S5B). Conversely, a significant enrichment of down-regulated DEGs was observed within the biological processes pertinent to antigen receptor-mediated signaling pathways and cell activation, indicative of a potential impairment in the immune function of B cells in PM (Fig. S5C).

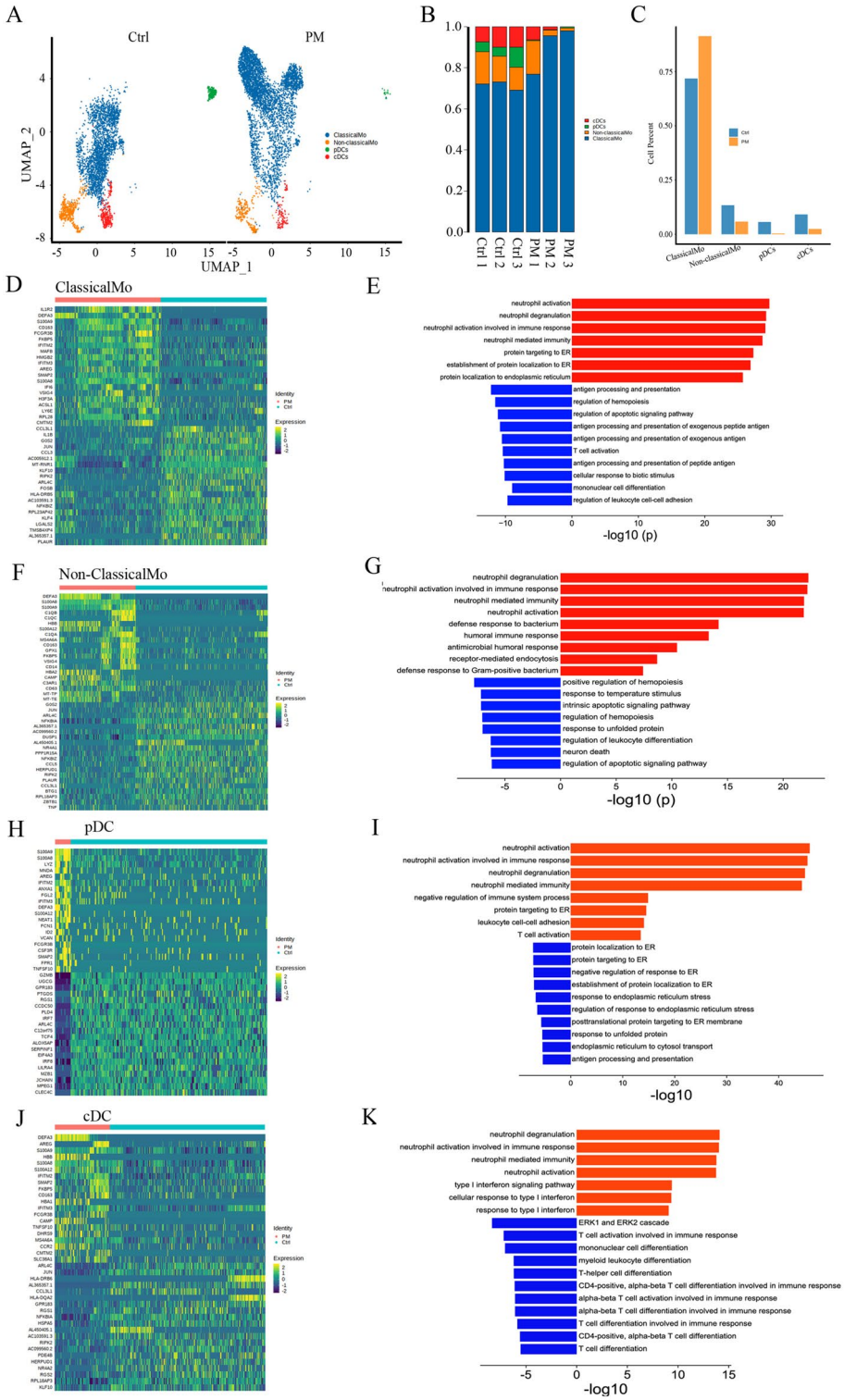

Further delineation of B cell subtypes was achieved by identifying and labeling characteristic genes specific to these subsets, leading to the classification of two primary subtypes: naïve B (NaïveB) cells and memory B (Bmem) cells (Fig. 7A). Notably, a distinct NaïveB cluster was observed to be uniquely present within the PM group. We next characterized NaiveB subsets and labeled them according to the typical genes of naïve B subsets, yielding five subsets of NaïveB cells (Fig. 7B). A comparative analysis of the proportions of naïve B cells between the PM and control groups is presented in Fig. 7C, with the Naïve 4 and Naïve 5 subsets being uniquely prominent in the PM cohort.

A subsequent in-depth functional characterization of the Naïve 4 and Naïve 5 subsets relative to other subsets was conducted. GO functional enrichment analysis revealed that the DEGs of the Naïve 4 subset were significantly enriched in processes such as neutrophil activation, phagocytosis, and T cell activation (Fig. 7D). KEGG analysis also revealed an enrichment of DEGs in both phagosome and chemokine signaling pathways (Fig. 7E). In the

◀**Fig. 4**. The immunological characteristics of myeloid cells in PM. (**A**) UMAP plot of myeloid subtypes (similar to Fig. 2A). (**B**) The relative proportions of myeloid subtypes in each sample. (**C**) Comparison of myeloid subtypes between PM and control groups. (**D**) Heatmap of DEGs in the ClassicalMO subtype between PM and control groups. (**E**) GO enrichment analysis of ClassicalMO DEGs between PM and control groups. (**F**) Heatmap of DEGs in the Non-ClassicalMO subtype between PM and control groups. (**G**) GO enrichment analysis of Non-ClassicalMO DEGs between PM and control groups. (**H**) Heatmap of DEGs in the pDC subtype between PM and control groups. (**I**) GO enrichment analysis of pDC DEGs between PM and control groups. (**J**) Heatmap of DEGs in the cDC subtype between PM and control groups. (**K**) GO enrichment analysis of cDC DEGs between PM and control groups. In panels (**E**), (**G**), (**I**) and (**K**), the red color indicates the pathways enriched by up-regulated DEGs, while the blue color indicates the pathways enriched by down-regulated DEGs. The vertical axis displays the enriched pathways. The length of the bars indicates the significance of the enrichment results, with longer bars representing more significant enrichment.

Naïve 5 subset, GO enrichment analysis pinpointed up-regulated DEGs, including *DEFA3, S100A12, LTF, CAMP*, and *PGLYRP1*, which are associated with neutrophil activation and antimicrobial humoral response pathways (Fig. 7F). The detailed information about GO and KEGG is presented in Supplementary Table S10.

Discussion

In this study, we comprehensively delved into the molecular characterization of immune cells within PBMCs from PM patients at the single-cell resolution. First, we observed an increase in the relative proportions of platelets, neutrophils, and proneutrophils and decreased proportions of NK cells, T cells, and pDCs in the PM group compared to the control group. Specifically, the platelet subtype 2 and Naïve 4 and 5 subsets were found to be unique to the PM group. Moreover, we identified the immunological features of different immune cells between the PM and the control groups. Our findings elucidated the multifaceted immune response, revealing both the activation of certain immune cells and the dampening of others, which may contribute to the pathogenesis of PM.

A large body of literature supports the function of platelets as key sentinel and effector cells in infectious diseases[37]. Here, we found an elevated platelet proportion in the PM group than in the control group, consistent with prior clinical studies showing relative increased platelet counts in pneumonia patients[8,9]. This correlation suggests that platelets may serve not only as a marker of disease severity but could also actively contribute to the pathophysiological cascades underlying PM. A novel aspect of our study is the identification of a unique platelet subtype (platelet subtype 2) in the PM group, characterized by an up-regulation in the IL6–JAK–STAT3 signaling pathway, which plays a critical role in megakaryopoiesis, platelet production, and maturation[34,38,39]. Importantly, IL6R, JAK1/2/3, and STAT3 were all up-regulated in platelet subtype 2. Previous studies have found that the inhibitor of the JAK/STAT3 pathway modulates platelet activation[39,40], emphasizing the role of STAT3 in modulating platelet production, maturation and activation[38]. Notably, the up-regulation of IL6R, JAK, and STAT3 in this subtype may actively promote platelet activation, which could have significant implications for the inflammatory processes within the central nervous system (CNS) during PM.

Furthermore, the up-regulated genes in platelets, such as *FCGR3B, FCGR2A, TLR4, TLR2*, and others, which are significantly enriched in the pathways that are related to neutrophil immunity, point to a synergistic relationship between platelets and neutrophils in PM. Platelets activate and recruit neutrophils through multiple interactions[41–44], while the recruited neutrophils, in turn, recognize activated platelets to initiate inflammatory responses[41]. This bidirectional crosstalk may amplify the immune response and may exacerbate inflammation and contribute to the immunopathology of PM.

Consistent with this, our results indicate a higher relative proportion of neutrophils and their precursors, proneutrophils, in the PM group compared to the control group. Their presence in PM appears to be a dual-faceted phenomenon. The elevated neutrophil counts observed are in alignment with their strategic deployment to the infection site, where they perform an indispensable role in the clearance of bacteria. However, the up-regulation of genes associated with neutrophil functions, such as *FPR1, FPR2, C5AR1, CXCR1, CXCR2*, and others, points to an overactive state that may contribute to the inflammatory cascade observed in PM. The activated platelets also amplify the immune response of neutrophils that release NETs[45,46]. These NETs, composed of neutrophil DNA and proteins, effectively trap and kill bacteria[47], yet their presence in the CNS during PM raises concerns. Notably, several up-regulated genes of both platelets and neutrophils in the PM group, such as *FCGR3B, FCGR2A, C5AR1, ITGAM, NCF4, TLR4*, and *TLR2,* are involved in NET formation, suggesting an elevated level of NET in PM. While NETs can be beneficial in trapping bacteria, their accumulation in the CSF may hinder the clearance of pneumococci and contribute to the inflammatory response. Some studies have proved that pneumococci can escape from NET-mediated killing, which promotes the spreading of pneumococci[48–50]. A recent study showed the presence of NETs in the CSF of PM patients, impairing pneumococcal clearance, emphasizing thetherapeutic potential of NET degradation[3]. Excessive NET formation has been associated with tissue damage and impaired bacterial clearance, suggesting a potential role in the pathogenesis of PM. The up-regulation of genes involved in NET formation and the interaction with platelets suggest a potential therapeutic target for modulating the inflammatory response in PM.

Another immunologic feature in the PM group is the relatively decreased proportion of NK cells, hinting at a deficiency in NK cell-mediated immunity. Currently, the precise role of NK cells in PM remains largely elusive. It is noteworthy that NK cells have been found to exacerbate *S. pneumoniae* infection by producing IL-10[51]. A 2005 study underscored that the elevated NK cell activity during pneumococcal

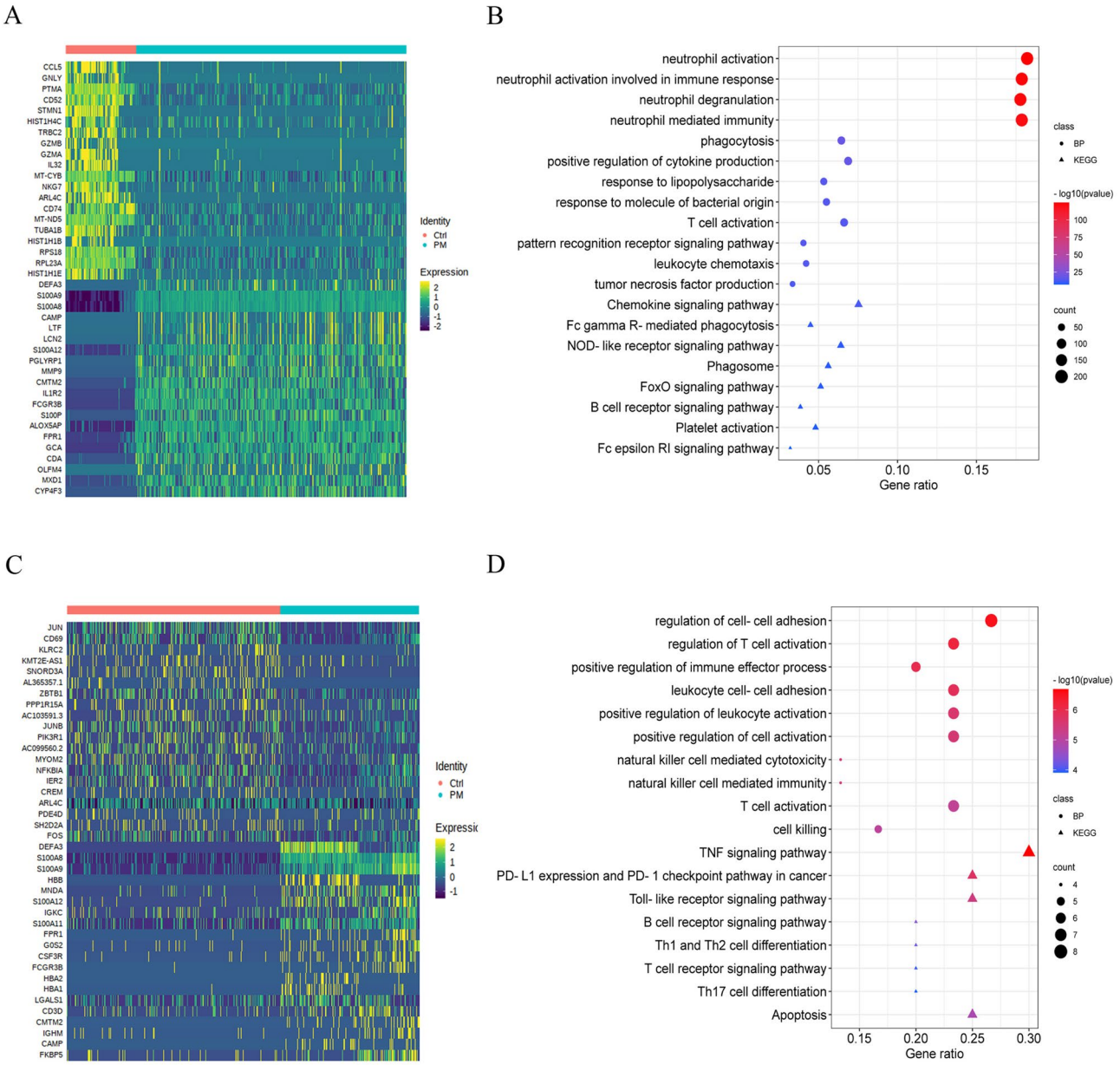

Fig. 5. The immunological characteristics of neutrophils/pro-neutrophils and NK cells in PM. (**A**) Heatmap of DEGs in neutrophils/pro-neutrophils between PM and control groups. (**B**) GO and KEGG enrichment analysis of neutrophils/pro-neutrophils DEGs between PM and control groups. Pathways are displayed on the vertical axis. At the bottom, the proportion of DEGs that are annotated to the pathway relative to the total number of DEGs is indicated. The size of the dot represents the ratio of the number of DEGs present in each pathway. The circle represents GO enrichment analysis, and the triangle represents KEGG enrichment analysis. (**C**) Heatmap of DEGs in NK cells between PM and control groups. (**D**) GO and KEGG enrichment analysis of NK cell DEGs between PM and control groups (similar to Fig. 5B).

pneumonia amplifies pulmonary and systemic inflammation, promotes bacteremia, and is associated with poor outcomes[13]. Additionally, Christaki et al. also demonstrated that NK cell depletion prolongs survival and suggested NK cells appear to contribute to mortality in pneumococcal pneumonia animal models with *S. pneumoniae* infection[14]. Furthermore, NK cells have been proven to regulate the adaptive immune response via stimulating or inhibiting the T cell response[52]. The relative decrease in NK cells observed in our study thus points to a possible deficiency in the adaptive immune response. This is further supported by the down-regulation of DEGs involved in T cell activation pathways.

Our analysis also revealed a unique subset of naïve B cells in PM patients. The up-regulation of genes related to neutrophil activation and antimicrobial humoral response pathways in these subsets suggests a potential role in the early innate immune response and its transition to adaptive immunity. Prior studies have proved that the

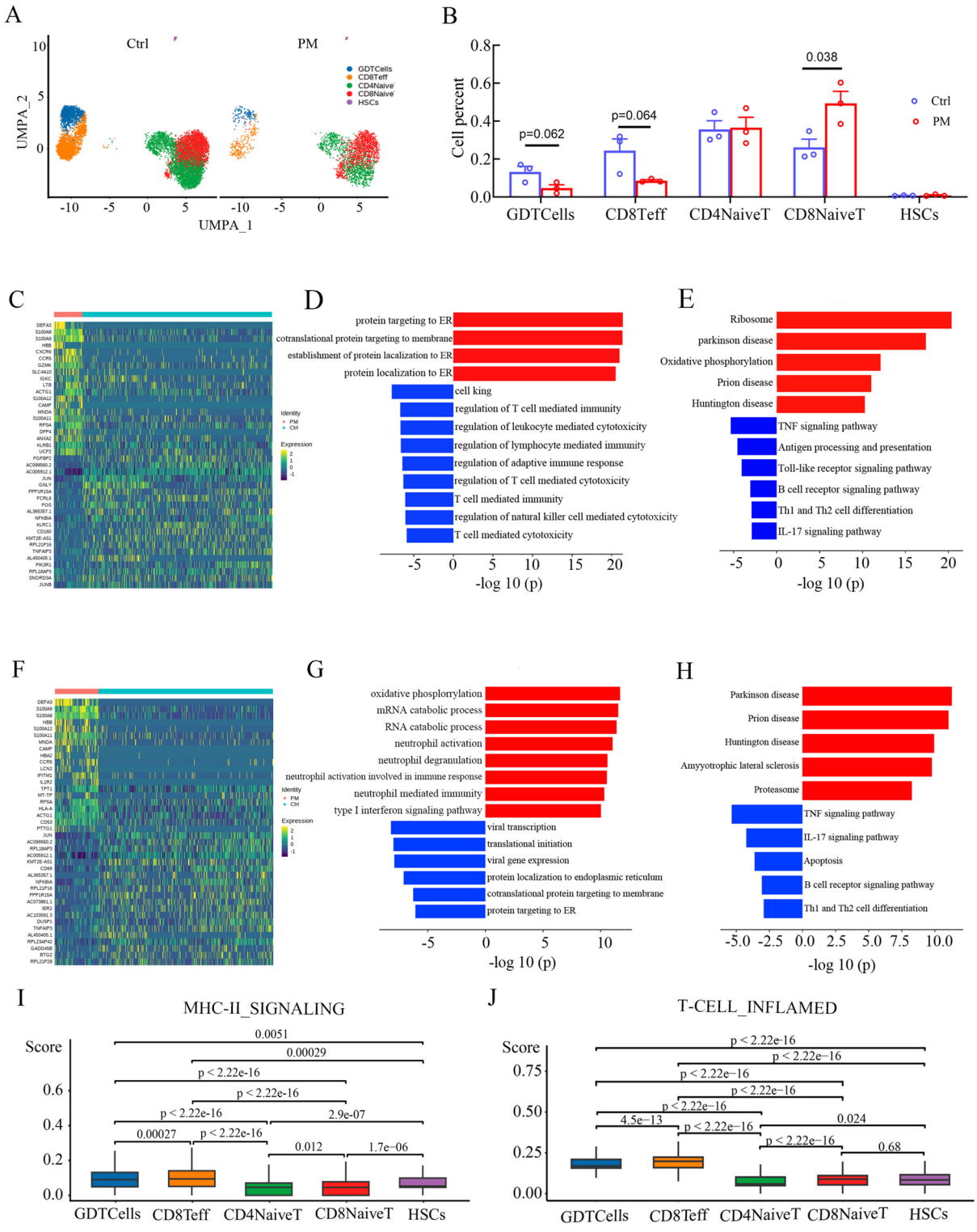

Fig. 6. The immunological characteristics of T cells in PM. (**A**) UMAP plot of T cell subtypes (similar to Fig. 2A). (**B**) The relative proportions of T cell subtypes in each individual. Comparisons were made using two-tailed unpaired Student's t test and the p-values are not adjusted for multiple comparisons. Data are shown as the mean ± SEM. (**C**) Heatmap of DEGs in the GDT subtype between PM and control groups. (**D**) GO enrichment analysis of GDT DEGs between PM and control groups (similar to Fig. 4). (**E**) KEGG enrichment analysis of GDT DEGs between PM and control groups (similar to Fig. 4). (**F**) Heatmap of DEGs in the CD8 + Teff subtype between PM and control groups. (**G**) GO enrichment analysis of CD8 + Teff DEGs between PM and control groups (similar to Fig. 4). (**H**) KEGG enrichment analysis of CD8 + Teff DEGs between PM and control groups (similar to Fig. 4). (**I**) Gene set analysis in the MHC-II signaling pathway. (**J**) Gene set analysis in the T-cell inflamed signaling pathway. For (**I**) and (**J**), Wilcoxon rank-sum test was performed, $p < 0.05$ was considered as statistically significant.

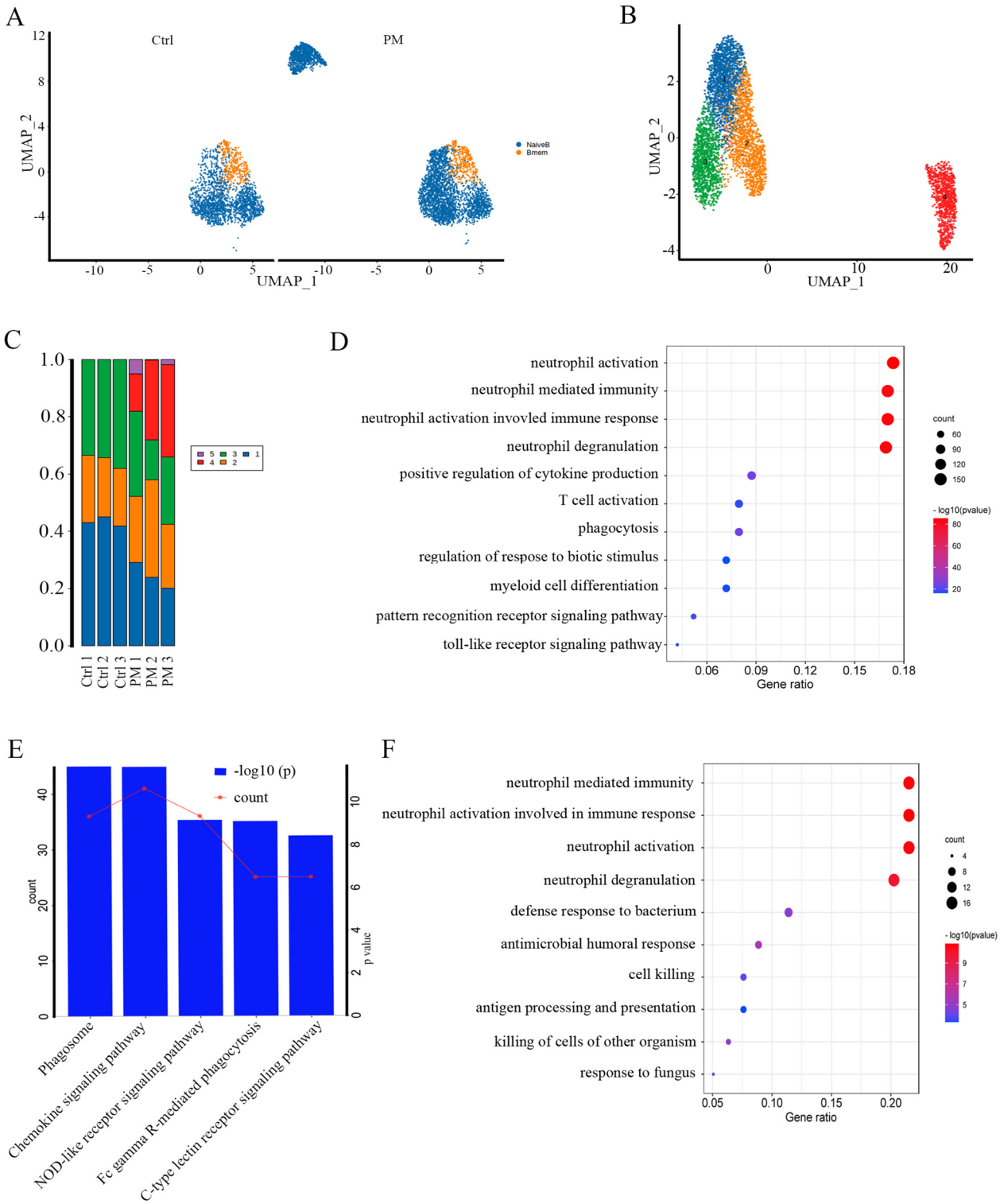

Fig. 7. The immunological characteristics of B cells in PM. (**A**) UMAP plot of B cell subtypes (similar to Fig. 2A). (**B**) UMAP plot of Naïve B cell subtypes (similar to Fig. 2A). (**C**) The relative proportions of Naïve B cell subtypes in each individual. (**D**) GO enrichment analysis of the Naïve B4 subset (similar to Fig. 2D). (**E**) KEGG enrichment analysis of the Naïve B4 subset (similar to Fig. 2E). (**F**) GO enrichment analysis of the Naïve B5 subset (similar to Fig. 2D).

neutrophils provide helper signals to B cells, generating an innate layer of antimicrobial immunoglobulin defense by interacting with the B cells[53,54]. The crosstalk between the innate and adaptive immune systems is crucial for the effective elimination of pathogens. However, the overall down-regulation of DEGs in B cells suggests an impaired function that may hinder the development of an effective antibody response. In addition, numerous genes that mediate antigen processing and presentation, as well as T cell activation pathway of myeloids, were down-regulated in the PM group compared with the control group. Specifically, the down-regulated DEGs of cDCs and pDCs in the PM group were enriched in the MHC-II protein complex, which suggested dysfunction in antigen processing and presentation. Furthermore, our study observed a significant relative decrease in the overall proportion of T cells, as well as the proportions of two subtypes GDT and CD8 Teff, in the PM group. The down-regulated DEGs of GDT cells in the PM group were enriched in T cell activation pathways, indicative of dysfunction of these T cell subsets. Previous animal studies have incontrovertibly proved that B and T cell deficiency result in a severe impairment of *S. pneumoniae* clearance and an exaggerated systemic inflammatory response[15].

In conclusion, our single-cell transcriptomic analysis of PM patients has provided novel insights into the immune cell dynamics and the potential dysregulation of immune pathways. The findings highlight the need for a more nuanced understanding of the immune response in PM, which could guide the development of targeted therapies. However, there were some limitations. The small sample size of six participants, including only one female, limits the generalizability of our findings and introduces potential biases related to sex-specific immune responses. Additionally, the identified emergent cell subsets could represent general cell states rather than novel types unique to the disease, necessitating further validation. Targeted investigations into specific cell types like neutrophils and B cells could also reveal more about their roles in disease progression. Further research is warranted to explore the mechanisms underlying the observed alterations in immune cell subsets and their implications for the treatment and prognosis of PM patients.

Our study acknowledges the presence of ambient RNA contamination, particularly in the Platelet-2 subset, which exhibits minimal expression of neutrophil markers. Similarly, Platelet-3 and Platelet-4 subsets show minimal expression of B-cell and T-cell markers, respectively. While this contamination does not significantly impact our overall clustering or major conclusions, it underscores the need for continued improvements in single-cell sequencing methodologies. As noted in the literature, complete elimination of contamination is often unattainable, highlighting that some level of contamination is an inherent challenge in single-cell RNA sequencing[55,56]. To address this, we performed re-clustering analyses after regressing out neutrophil-specific genes and other contaminant genes, confirming the robustness of our findings (Fig. S2D and S2E). Future work should focus on adopting advanced technologies, such as droplet-based single-cell sequencing and improved cell labeling methods, as well as implementing stricter bioinformatics strategies to further refine cell subset identification and reduce the influence of contaminants.

Data availability

The datasets presented in this study can be found in the National Genomics Data Center with the accession number(s) HRA009106. The datasets used and/or analyzed during the current study are available from the corresponding author on reasonable request.

Received: 9 October 2024; Accepted: 12 May 2025
Published online: 22 May 2025

References

1. Hathaway, L. J. New virulence factors identified in pneumococcal meningitis. *Trends Microbiol.* **27**, 895–896. https://doi.org/10.1016/j.tim.2019.08.008 (2019).
2. Darmaun, L., Levy, C., Lagree, M., Bechet, S., Varon, E., Dessein, R., Cohen, R., Martinot, A., Dubos, F. & A.-G.S. Group. Recurrent pneumococcal meningitis in children: A multicenter case–control study. Pediatr. Infect. Dis. J. **38**, 881–886. https://doi.org/10.1097/INF.0000000000002358 (2019).
3. Mohanty, T. et al. Neutrophil extracellular traps in the central nervous system hinder bacterial clearance during pneumococcal meningitis. *Nat. Commun.* **10**, 1667. https://doi.org/10.1038/s41467-019-09040-0 (2019).
4. Brooks, L. R. K. & Mias, G. I. *Streptococcus pneumoniae*'s Virulence and Host Immunity: Aging. *Diagn. Prev. Front. Immunol.* **9**, 1366. https://doi.org/10.3389/fimmu.2018.01366 (2018).
5. Jedrzejas, M. J. Pneumococcal virulence factors: Structure and function. *Microbiol. Mol. Biol. Rev.* **65**, 187–207. https://doi.org/10.1128/MMBR.65.2.187-207.2001 (2001).
6. Koedel, U., Klein, M. & Pfister, H. W. New understandings on the pathophysiology of bacterial meningitis. *Curr. Opin. Infect. Dis.* **23**, 217–223. https://doi.org/10.1097/QCO.0b013e328337f49e (2010).
7. Polfliet, M. M. et al. Meningeal and perivascular macrophages of the central nervous system play a protective role during bacterial meningitis. *J. Immunol.* **167**, 4644–4650. https://doi.org/10.4049/jimmunol.167.8.4644 (2001).
8. Sahin, M., Duru, N. S., Elevli, M. & Civilibal, M. Assessment of platelet parameters in children with pneumonia. *J. Pediatr. Infect.* **11**, 122–128. https://doi.org/10.5578/ced.201732 (2017).
9. Prina, E. et al. Thrombocytosis is a marker of poor outcome in community-acquired pneumonia. *Chest* **143**, 767–775. https://doi.org/10.1378/chest.12-1235 (2013).
10. Cundell, D. R., Gerard, N. P., Gerard, C., Idanpaan-Heikkila, I. & Tuomanen, E. I. *Streptococcus pneumoniae* anchor to activated human cells by the receptor for platelet-activating factor. *Nature* **377**, 435–438. https://doi.org/10.1038/377435a0 (1995).
11. Auburtin, M. et al. Pneumococcal meningitis in the intensive care unit: prognostic factors of clinical outcome in a series of 80 cases. *Am. J. Respir. Crit. Care Med.* **165**, 713–717. https://doi.org/10.1164/ajrccm.165.5.2105110 (2002).
12. Wasier, A. P. et al. Pneumococcal meningitis in a pediatric intensive care unit: Prognostic factors in a series of 49 children. *Pediatr. Crit. Care Med.* **6**, 568–572. https://doi.org/10.1097/01.pcc.0000170611.85012.01 (2005).
13. Kerr, A. R. et al. Identification of a detrimental role for NK cells in pneumococcal pneumonia and sepsis in immunocompromised hosts. *Microbes Infect.* **7**, 845–852. https://doi.org/10.1016/j.micinf.2005.02.011 (2005).
14. Christaki, E. et al. NK and NKT cell depletion alters the outcome of experimental pneumococcal pneumonia: Relationship with regulation of interferon-gamma production. *J. Immunol. Res.* **2015**, 532717. https://doi.org/10.1155/2015/532717 (2015).

15. Ribes, S. et al. The early adaptive immune response in the pathophysiological process of pneumococcal meningitis. *J. Infect. Dis.* **215**, 150–158. https://doi.org/10.1093/infdis/jiw517 (2017).
16. Ivanov, S., Paget, C. & Trottein, F. Role of non-conventional T lymphocytes in respiratory infections: The case of the pneumococcus. *PLoS Pathog.* **10**, e1004300. https://doi.org/10.1371/journal.ppat.1004300 (2014).
17. Ercoli, G. et al. The influence of B cell depletion therapy on naturally acquired immunity to *Streptococcus pneumoniae*. *Front. Immunol.* **11**, 611661. https://doi.org/10.3389/fimmu.2020.611661 (2020).
18. Ramos-Sevillano, E., Ercoli, G. & Brown, J. S. Mechanisms of naturally acquired immunity to *Streptococcus pneumoniae*. *Front. Immunol.* **10**, 358. https://doi.org/10.3389/fimmu.2019.00358 (2019).
19. Brown, J. S. et al. The classical pathway is the dominant complement pathway required for innate immunity to *Streptococcus pneumoniae* infection in mice. *Proc. Natl. Acad. Sci. USA* **99**, 16969–16974. https://doi.org/10.1073/pnas.012669199 (2002).
20. Dura, B. et al. scFTD-seq: freeze-thaw lysis based, portable approach toward highly distributed single-cell 3' mRNA profiling. *Nucleic Acids Res.* **47**, e16. https://doi.org/10.1093/nar/gky1173 (2019).
21. Martin, M. Cutadapt removes adapter sequences from high-throughput sequencing reads. *EMBnet J.* **17**, 10–12 (2011).
22. Dobin, A. et al. STAR: Ultrafast universal RNA-seq aligner. *Bioinformatics* **29**, 15–21. https://doi.org/10.1093/bioinformatics/bts635 (2013).
23. Liao, Y., Smyth, G. K. & Shi, W. featureCounts: An efficient general purpose program for assigning sequence reads to genomic features. *Bioinformatics* **30**, 923–930. https://doi.org/10.1093/bioinformatics/btt656 (2014).
24. Satija, R., Farrell, J. A., Gennert, D., Schier, A. F. & Regev, A. Spatial reconstruction of single-cell gene expression data. *Nat. Biotechnol.* **33**, 495–502. https://doi.org/10.1038/nbt.3192 (2015).
25. Korsunsky, I. et al. Fast, sensitive and accurate integration of single-cell data with Harmony. *Nat. Methods* **16**, 1289–1296. https://doi.org/10.1038/s41592-019-0619-0 (2019).
26. Yu, G., Wang, L. G., Han, Y. & He, Q. Y. clusterProfiler: An R package for comparing biological themes among gene clusters. *OMICS* **16**, 284–287. https://doi.org/10.1089/omi.2011.0118 (2012).
27. Kanehisa, M. & Goto, S. KEGG: kyoto encyclopedia of genes and genomes. *Nucleic Acids Res.* **28**, 27–30. https://doi.org/10.1093/nar/28.1.27 (2000).
28. Kanehisa, M. Toward understanding the origin and evolution of cellular organisms. *Protein Sci.* **28**, 1947–1951. https://doi.org/10.1002/pro.3715 (2019).
29. Kanehisa, M., Furumichi, M., Sato, Y., Kawashima, M. & Ishiguro-Watanabe, M. KEGG for taxonomy-based analysis of pathways and genomes. *Nucleic Acids Res.* **51**, D587–D592. https://doi.org/10.1093/nar/gkac963 (2023).
30. Qiu, X. et al. Single-cell mRNA quantification and differential analysis with Census. *Nat. Methods* **14**, 309–315. https://doi.org/10.1038/nmeth.4150 (2017).
31. Gulati, G. S. et al. Single-cell transcriptional diversity is a hallmark of developmental potential. *Science* **367**, 405–411. https://doi.org/10.1126/science.aax0249 (2020).
32. Andreatta, M. & Carmona, S. J. UCell: Robust and scalable single-cell gene signature scoring. *Comput. Struct. Biotechnol. J.* **19**, 3796–3798. https://doi.org/10.1016/j.csbj.2021.06.043 (2021).
33. Nicolai, L. & Massberg, S. Platelets as key players in inflammation and infection. *Curr. Opin. Hematol.* **27**, 34–40. https://doi.org/10.1097/moh.0000000000000551 (2020).
34. Chen, K., Rondina, M. T. & Weyrich, A. S. A sticky story for signal transducer and activator of transcription 3 in platelets. *Circulation* **127**, 421–423. https://doi.org/10.1161/CIRCULATIONAHA.112.155366 (2013).
35. Shegarfi, H. et al. The role of natural killer cells in resistance to the intracellular bacterium Listeria monocytogenes in rats. *Scand. J. Immunol.* **70**, 238–244. https://doi.org/10.1111/j.1365-3083.2009.02292.x (2009).
36. Abel, A. M., Yang, C., Thakar, M. S. & Malarkannan, S. Natural killer cells: Development, maturation, and clinical utilization. *Front. Immunol.* **9**, 1869. https://doi.org/10.3389/fimmu.2018.01869 (2018).
37. Guo, L. & Rondina, M. T. The era of thromboinflammation: Platelets are dynamic sensors and effector cells during infectious diseases. *Front. Immunol.* **10**, 2204. https://doi.org/10.3389/fimmu.2019.02204 (2019).
38. Zhou, Z. et al. Signal transducer and activator of transcription 3 (STAT3) regulates collagen-induced platelet aggregation independently of its transcription factor activity. *Circulation* **127**, 476–485. https://doi.org/10.1161/CIRCULATIONAHA.112.132126 (2013).
39. Lu, W. J. et al. Role of a Janus kinase 2-dependent signaling pathway in platelet activation. *Thromb. Res.* **133**, 1088–1096. https://doi.org/10.1016/j.thromres.2014.03.042 (2014).
40. Xu, Z. et al. A novel STAT3 inhibitor negatively modulates platelet activation and aggregation. *Acta Pharmacol. Sin.* **38**, 651–659. https://doi.org/10.1038/aps.2016.155 (2017).
41. Sreeramkumar, V. et al. Neutrophils scan for activated platelets to initiate inflammation. *Science* **346**, 1234–1238. https://doi.org/10.1126/science.1256478 (2014).
42. Duerschmied, D. et al. Platelet serotonin promotes the recruitment of neutrophils to sites of acute inflammation in mice. *Blood* **121**, 1008–1015. https://doi.org/10.1182/blood-2012-06-437392 (2013).
43. Miedzobrodzki, J. et al. Platelets augment respiratory burst in neutrophils activated by selected species of gram-positive or gram-negative bacteria. *Folia Histochem Cytobiol* **46**, 383–388. https://doi.org/10.2478/v10042-008-0052-1 (2008).
44. Rahman, M. et al. Platelet-derived CD40L (CD154) mediates neutrophil upregulation of Mac-1 and recruitment in septic lung injury. *Ann. Surg.* **250**, 783–790. https://doi.org/10.1097/SLA.0b013e3181bd95b7 (2009).
45. Carestia, A. et al. Mediators and molecular pathways involved in the regulation of neutrophil extracellular trap formation mediated by activated platelets. *J. Leukoc. Biol.* **99**, 153–162. https://doi.org/10.1189/jlb.3A0415-161R (2016).
46. Caudrillier, A. et al. Platelets induce neutrophil extracellular traps in transfusion-related acute lung injury. *J. Clin. Invest.* **122**, 2661–2671. https://doi.org/10.1172/JCI61303 (2012).
47. Brinkmann, V. et al. Neutrophil extracellular traps kill bacteria. *Science* **303**, 1532–1535. https://doi.org/10.1126/science.1092385 (2004).
48. Beiter, K. et al. An endonuclease allows *Streptococcus pneumoniae* to escape from neutrophil extracellular traps. *Curr. Biol.* **16**, 401–407. https://doi.org/10.1016/j.cub.2006.01.056 (2006).
49. Jhelum, H., Sori, H. & Sehgal, D. A novel extracellular vesicle-associated endodeoxyribonuclease helps *Streptococcus pneumoniae* evade neutrophil extracellular traps and is required for full virulence. *Sci. Rep.* **8**, 7985. https://doi.org/10.1038/s41598-018-25865-z (2018).
50. Storisteanu, D. M. et al. Evasion of neutrophil extracellular traps by respiratory pathogens. *Am. J. Respir. Cell Mol. Biol.* **56**, 423–431. https://doi.org/10.1165/rcmb.2016-0193PS (2017).
51. Clark, S. E., Schmidt, R. L., Aguilera, E. R. & Lenz, L. L. IL-10-producing NK cells exacerbate sublethal *Streptococcus pneumoniae* infection in the lung. *Transl. Res.* **226**, 70–82. https://doi.org/10.1016/j.trsl.2020.07.001 (2020).
52. Crouse, J., Xu, H. C., Lang, P. A. & Oxenius, A. NK cells regulating T cell responses: Mechanisms and outcome. *Trends Immunol.* **36**, 49–58. https://doi.org/10.1016/j.it.2014.11.001 (2015).
53. Puga, I. et al. B cell-helper neutrophils stimulate the diversification and production of immunoglobulin in the marginal zone of the spleen. *Nat. Immunol.* **13**, 170–180. https://doi.org/10.1038/ni.2194 (2011).
54. Cerutti, A., Puga, I. & Magri, G. The B cell helper side of neutrophils. *J. Leukoc. Biol.* **94**, 677–682. https://doi.org/10.1189/jlb.1112596 (2013).
55. Ba, R. et al. FOXG1 drives transcriptomic networks to specify principal neuron subtypes during the development of the medial pallium. *Sci. Adv.* **9**, eade2441. https://doi.org/10.1126/sciadv.ade2441 (2023).

56. Jakel, S. et al. Altered human oligodendrocyte heterogeneity in multiple sclerosis. *Nature* **566**, 543–547. https://doi.org/10.1038/s41586-019-0903-2 (2019).
57. Zhang, Y., Duan, J., Lin, S., Wen, J., & Liao, J. https://doi.org/10.21203/rs.3.rs-1834120/v1 (2022).

Acknowledgements
We thank all three patients and three healthy individuals, as well as their patients or surrogates for their invaluable participation in this experiment. We also acknowledge with deep appreciation the nurses from Shenzhen Children's Hospital for their diligent efforts in collecting the samples. We are delighted to announce that the manuscript has been preprinted and is now available online [57].

Author contributions
JL conceived and designed the study. JL and YZ analyzed the data and wrote the manuscript. JD collected the sample. SL and JW participated in the study design and interpretation of data.

Funding
This work is supported by Shenzhen Fund (JCYJ20200109150818777, JCYJ20220530160001002), Sanming Project of Medicine in Shenzhen (SZSM202311028, SZSM201812005), Shenzhen Fund for Guangdong Provincial High Level Clinical Key Specialties (No. SZGSP012), Basic and Applied Basic Research Fund Committee of Guangdong Province (2020A1515110612), and Guangdong High-level Hospital Construction Fund (ynkt2021-zz24).

Declarations

Competing interests
The authors declare no competing interests.

Consent for publication
All authors read and approved the final manuscript for publication.

Additional information
Supplementary Information The online version contains supplementary material available at https://doi.org/10.1038/s41598-025-02258-7.

Correspondence and requests for materials should be addressed to J.L.

Reprints and permissions information is available at www.nature.com/reprints.

Publisher's note Springer Nature remains neutral with regard to jurisdictional claims in published maps and institutional affiliations.